Irreversible effects of drying-wetting cycles on shrinkage and water retention of compacted London clay

Ana Sofia Dias[1*], *Paul* Hughes[1], and *David* Toll[1]

[1]Department of Engineering, Durham University, DH1 3LE Durham, UK

Abstract. Long-linear assets, such as roads and railways, supported by earthworks are susceptible to deterioration caused by weather cycles, that translate into changes in soil hydro-mechanical properties. Failures in these earthworks are expected to become more common due to climate change as periods of drought and extreme rainfall events become more frequent. In the present study, the effect of the suction range of the moisture cycle on the soil-water retention curve (SWRC) and soil shrink-swell curve (SSC) of active London clay is investigated. Soil samples compacted at Proctor optimum conditions were subjected to drying-wetting cycles within a variable suction interval. A change in the SSC was observed when the water content reduced below a threshold that approximates to the shrinkage limit. A reduction in the ability of the soil to hold suction was observed with SWRCs becoming less steep, as the Primary Drying Line was steeper than subsequent drying phases (Scanning Drying Lines). Once the Scanning Drying Line intersects the Primary Drying Line, a yielding point is identified, and the soil loses further ability to hold suction. Irreversible deformations were observed associated with changes in the SWRC from drying-wetting cycles.

1 Introduction

Embankments constructed using active clays, such as London Clay, are part of the key transport infrastructure on which the UK relies. However, active clays are susceptible to volumetric deformations caused by variations of water content induced by the weather. The volumetric deformations in these embankments affect the performance of the transport infrastructure, in particular, the railways due to their sensitivity to the track deformations [1], and may lead to failure [2, 3].

Moisture cycles in the ground are becoming more extreme as a consequence of more frequent and more extreme weather events caused by the climate change. The performance of the transport infrastructure has the potential to be extensively affected by climate change as the soil properties deteriorate [4, 5]. Cycles of wetting and drying result in change in the soil hydraulic properties [6, 7], accumulation of deformations [8, 9], and reduction of strength [5]. These changes have the potential to be amplified with more extreme moisture cycles.

In order to understand the behaviour of earthworks in a climate change context, a study of the effect of extreme moisture cycles needs to be undertaken. The present study focuses on the evolution of the Soil-Water Retention Curve (SWRC) and Soil Shrinkage Curve (SSC) of an active clay subjected to different ranges of moisture cycles.

Previous studies have shown that cycles of drying and wetting result in a shift of the SWRC towards lower suctions, which translates into a reduction of the soil strength [5]. The moisture cycling also results in accumulation of deformations explained by the particle rearrangement [8, 10], and fatigue behaviour has been observed [11, 12]. However, the effect of the increase in the moisture cycle range and the accumulation of irreversible deformations with increasing number of cycles is not yet well understood.

2 Methods and materials

2.1 Soil properties and sample preparation

The present work focused on the study of London Clay collected from Clapham (London, UK), for which properties are summarised in Table 1. The characterization was performed following the British Standard [13], according to which the soil was classified as high plasticity clay.

Three samples were statically compacted at optimum water content (w = 22%) and maximum dry density (γ_d = 1.58Mg/m^3) according to the Proctor compaction test [13] as previously determined [14]. The samples #1 and #2 were subjected to suction changes above 1 MPa, while sample #3 was subjected to suction changes below 1 MPa. The dimensions of the samples were conditioned by the adopted methods to measure suction. Samples #1 and #2 were compacted in a cylindrical mould to a diameter of 15 mm and a height of 5 mm. Sample #3 was compacted to a dimeter of 100 mm and a height of 20 mm. The properties (void ratio, water content, and suction) of the samples at compaction are reported in Table 2. The suction at compaction on

* Corresponding author: author@email.org

sample #3 was not measured but it is expected to be within the values measured on samples #1 and #2.

Table 1. London clay classification properties [13].

Specific gravity		2.77
Particle size fractions	Clay	57%
	Silt	36%
	Sand	8%
Atterberg limits	Liquid limit	60%
	Plasticity index	36%

Table 2. Samples' properties at compaction (suction range of testing; void ratio, e; water ratio, e_w; degree of saturation, S_r; and suction, s).

#	Suction range	e	e_w	S_r	s (MPa)
1	> 1 MPa	0.76	0.61	0.80	1.46
2	> 1 MPa	0.82	0.59	0.72	1.66
3	< 1 MPa	0.80	0.61	0.76	-

2.2 Soil-water retention curve measurements above 1 MPa

Samples #1 and #2 were subjected to cycles of drying and wetting of different range. During the cycling, the total suction was measured using a chilled mirror dew point potentiameter WP4C (by METER Group, Inc.). The samples were weighed using a balance with a precision of 0.0001g, due to being small (weighing between 1.4 and 1.8 g), and the diameter and height of the samples were measured twice using a calliper with an accuracy of 0.01 mm. On these samples, the cycles were performed over a range of total suction between 1 MPa and a variable maximum total suction upon drying, which is reported in Figure 1.

The drying of the samples was performed by being exposed to the laboratory environment for approximately 5 minutes. The wetting process was performed by adding approximately 0.01 to 0.02g of distilled water to the top of the sample with the help of a syringe. In both cases (drying and wetting), the samples were sealed in air-tight containers for at least 30 minutes to allow the water to redistribute within the sample before the measurements were performed (dimensions, weight, and total suction).

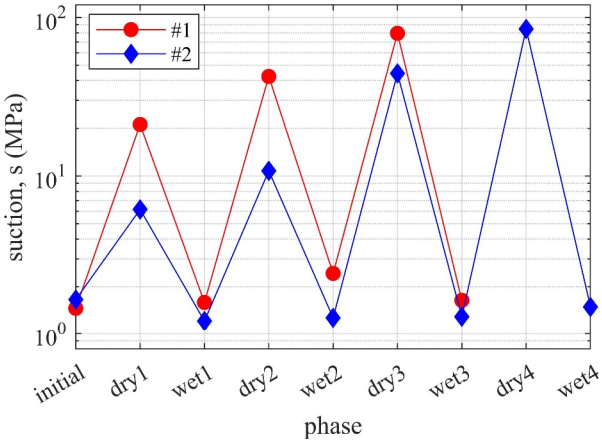

Fig. 1. Suction range imposed on samples #1 and #2.

2.3 Soil-water retention curve measurements below 1 MPa

Sample #3, which was compacted at the same conditions as the remaining samples, was subjected to three cycles of wetting and drying between 0.01 and 1 MPa of matric suction.

The Durham Soil Water Retention Apparatus was used to monitor the sample [15, 16]. This apparatus is equipped with six displacement transducers to measure deformations in cylindrical soil samples (diameter and height). The matric suction was measured using a high capacity tensiometer installed at the base of the sample. The changes of the sample's weight were recorded by a balance with a precision of 0.01 g, as this sample's weight varied between 324 and 290 g. All measurements were automatically recorded every 5 minutes by a datalogger.

The wetting was imposed by adding water to the top of the sample using four syringe pumps at a regular time interval. The suction was not recorded during the wetting phases. The drying phase was obtained by allowing water to evaporate from the exposed surfaces of the sample, however, the sample was always covered to limit the air flow and to slow down the drying process.

2.4 Representation of results: soil-water retention curves and soil shrink curve

The Soil-Water Retention Curve (SWRC) in the present study was represented in terms of suction (s) versus water ratio (e_w) or degree of saturation (S_r). The water ratio is given by the volume of water divided by the volume of soil particles, for which the water ratio is related to the void ratio and degree of saturation through Equation 1. It also represents gravimetric water content (w) scaled by specific gravity (G_s).

$$e_w = S_r \cdot e = w \cdot G_s \quad (1)$$

The Soil Shrinkage Curve (SSC) was represented in the present study in terms of void ratio (e) versus water ratio (e_w) or versus suction (s).

It is worth noting that the suction measured using the WP4C is total suction and the suction measured by the tensiometer is matric suction. The total suction is a sum

of the matric suction (due to capillary forces) with the osmotic suction (due to salts dissolved in the pore-water). In the analysis of results in the present study, the osmotic component was disregarded, as is common for the high suction range.

3 Results

3.1 Soil shrinkage curves

3.1.1 Analysis of the soil shrinkage curves

Figure 2 shows the SSCs of samples #1 and #2 overlapped with the SSCs of sample #3 to evaluate the soil shrinkage behaviour over a wide water content range. Three zones along the SSC can be identified in the SSCs, which are (from wet to dry): (i) the proportional shrinkage; (ii) the residual shrinkage; and (iii) the zero-shrinkage [17].

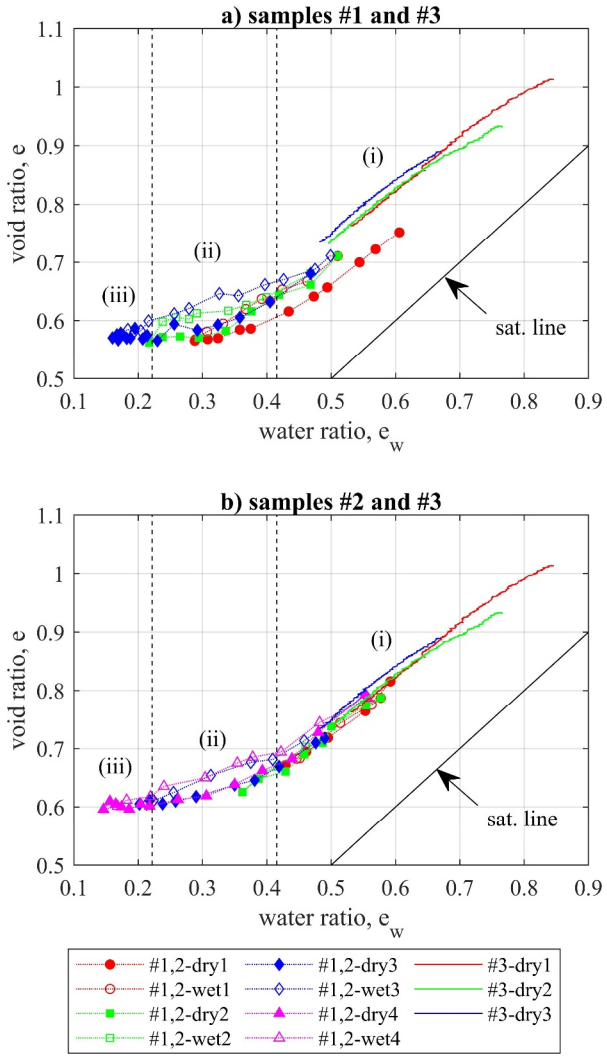

Fig. 2. Soil shrinkage curves of samples #1, #2, and #3.

The proportional shrinkage zone of the SSC is parallel to the saturation line, which is when the void ratio is equal to the water ratio (1:1, in Fig. 2). Therefore, in this zone, the void ratio changes approximately proportionally to the water ratio at an equal rate, given by Equation 2.

$$\partial e/\partial e_w \approx 1 \quad (2)$$

As the rate of the change of void ratio decreases, the residual shrinkage zone initiates, when Eq. 2 no longer holds, until no further volumetric deformations occur reaching a minimum void ratio that characterizes the zero-shrinkage zone. The shrinkage limit occurs within the residual shrinkage zone and can be determined by the intercept of a line tangent to the proportional shrinkage portion and minimum void ratio of the zero-shrinkage portion.

The SSCs of sample #3 show part of the proportional shrinkage zone, while the SSC of samples #1 and #2 initiate at end of the proportional shrinkage zone and end within the residual or the zero-shrinkage zone (Fig. 2).

3.1.2 Evolution of the soil shrinkage curve

The drying-wetting cycles imposed on the samples lead to a change of the SSCs which can be observed in some cycles (Fig. 2). Sample #3, that was subjected to cycles of suction bellow 1 MPa, did not present changes with increasing number of cycles. The SSC did not change slope and the no consistent shift of the position of the curve was identified. These SSCs presented a typical behaviour of the proportional shrinkage zone. Also in the first and second cycles imposed on sample #2, no changes were observed when compared with the first drying SSC. The maximum suction reached upon the first and second drying phases were 6MPa and 11MPa, respectively (Fig. 1), and the water content variation occurred within the proportional shrinkage zone and the initial portion of the residual shrinkage zone.

For samples #1 and #2, the SSCs obtained by drying the soil up to a maximum suction exceeding 21 MPa showed changes with increasing number of cycles. These SSCs shifted further away from the saturation line. Yet, the shift in sample #2 is less noticeable than the shift observed for sample #1. As a consequence of the shift of the SSCs, the shrinkage limit propagates towards lower water content values and volumetric deformations occur until progressively lower water contents but at the same rate as in previous cycles.

A shift of the SSCs away from the saturation line has been observed in previous studies [12, 18]. Nonetheless, in Figure 2, the shift in the SSC seems to indicate dependency on the range of the drying-wetting cycle imposed on the soil. This is, greater shifts in the SSC further away from the saturation line occur after a the soil had been dried to a lower water ratio. If the soil is dried and wetted within a given range of water ratio, no shift occurs in the SSC and the deformations are reversible. The threshold that separates the reversible from the irreversible deformations cannot be accurately identified with the data reported in the present study but the measurements indicate that the threshold is within the residual shrinkage zone because the drying-wetting cycles performed within the proportional shrinkage zone were reversible. The threshold could be associated with

the shrinkage limit, which falls within the residual shrinkage zone, as it was observed that drying-wetting cycles that exceeded the shrinkage limit resulted in a shift of the SSC further away from the saturation line.

When the drying-wetting cycle occurs within the proportional shrinkage zone, no propagation of the SSC was observed. However, when the minimum water content reached upon drying was below a particular threshold, the SSC moved further away from the saturation line.

3.2 Soil-water retention curves

3.2.1 Soil-water retention curves independent of volume deformations

The SWRCs represented in terms of suction versus water ratio, which do not account for volumetric deformations, are presented in Figure 3. A Primary Drying Line (PDL) can be identified in the SWRCs of samples #1 and #2 (Fig. 3a,b) as upon increasing number of cycles an upper boundary is established above which no soil state is possible [19]. A linear regression in the semi-log plane is presented with the respective coefficient of determination (R^2). A linear function in the semi-log plane was observed to represent the SWRCs in range of measurements reported in the present study when presented in terms of water ratio. Both samples #1 and #2 presented the same PDL as the fitting parameters are very similar.

The subsequent drying SWRCs present an initial less steep change of the water ratio with suction before intersecting the PDL at the yielding point, which will be here referred as Scanning Drying Line (SDL), representing a scanning curve below the PDL. The SDL of different drying phases are parallel and their position dependent on the initial water ratio. The mean and standard deviation of the slope of these SDLs is presented in Table 3 for each sample. The slope was determined for the relation between the logarithm of base 10 of the suction in MPa and the water ratio.

Table 3. Slope of the linear regression fitted to the scanning branch of the drying SWRCs in a x-log scale in which suction is represented in MPa ($\log_{10}$).

Sample	Mean	Standard deviation
#1	-0.188	0.002
#2	-0.198	0.044
#3	-0.137	0.027

The wetting SWRCs are also parallel and their position depends on the maximum suction reached upon drying, following a different path from the SDLs due to hysteresis. Therefore, cycles in which the maximum suction reached upon drying is higher are characterized by lower suctions during wetting, which propagate with subsequent cycling. This is particularly evident for sample #2, where the SDL shifts towards lower suction values with increasing number of cycles.

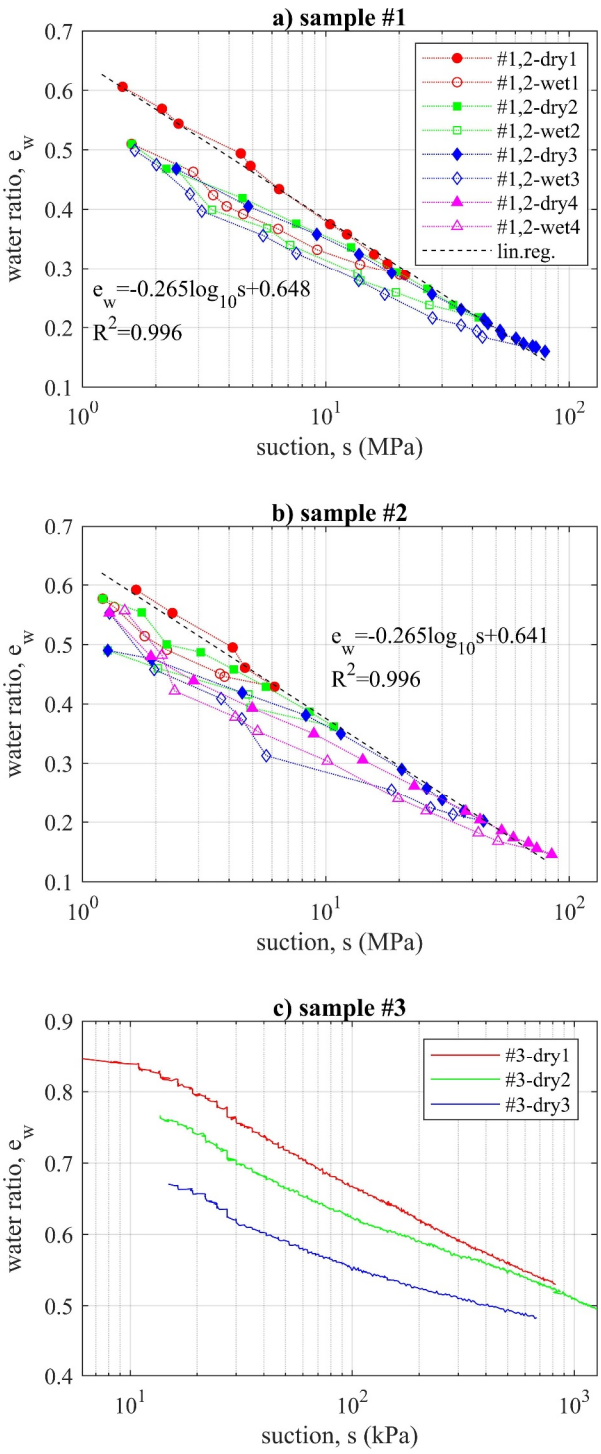

Fig. 3. Soil water retention curves in terms of water ratio of samples #1, #2, and #3.

The SWRCs of sample #3 present a progressive shift towards lower suction values with increasing number of cycles (Fig. 3c). The slope of the SWRCs approximates the slope of the SDLs of samples #1 and #2 more than of the PDL, as observed in Table 3. Therefore, the SWRCs of sample #3 could be assumed to be SDLs which propagate towards lower suction values as a consequence of the increase of the maximum suction

reached upon the previous drying and a decrease of the water content reached upon wetting.

Evidence of SWRCs shifting towards lower suctions has been observed in previous studies when the water content exchange involves capillary water [7], which is similar to what is observed on sample #3 (Fig. 3c). The shape of the SWRC depends on the compaction conditions for water contents above the threshold that separates water exchanges involving adsorbed water (intra-aggregate water) from capillary water (inter-aggregate water) [20, 21].

3.2.2 Evolution of the soil-water retention curves

In Figure 4, following the interpretation of the SWRC proposed by Toll [19], the SWRCs and the SSCs are represented simultaneously, but only the drying curves are shown to improve clarity. In Figure 5, the SWRCs are represented in terms of degree of saturation, where the changes in void ratio are taken into account (Eq. 1).

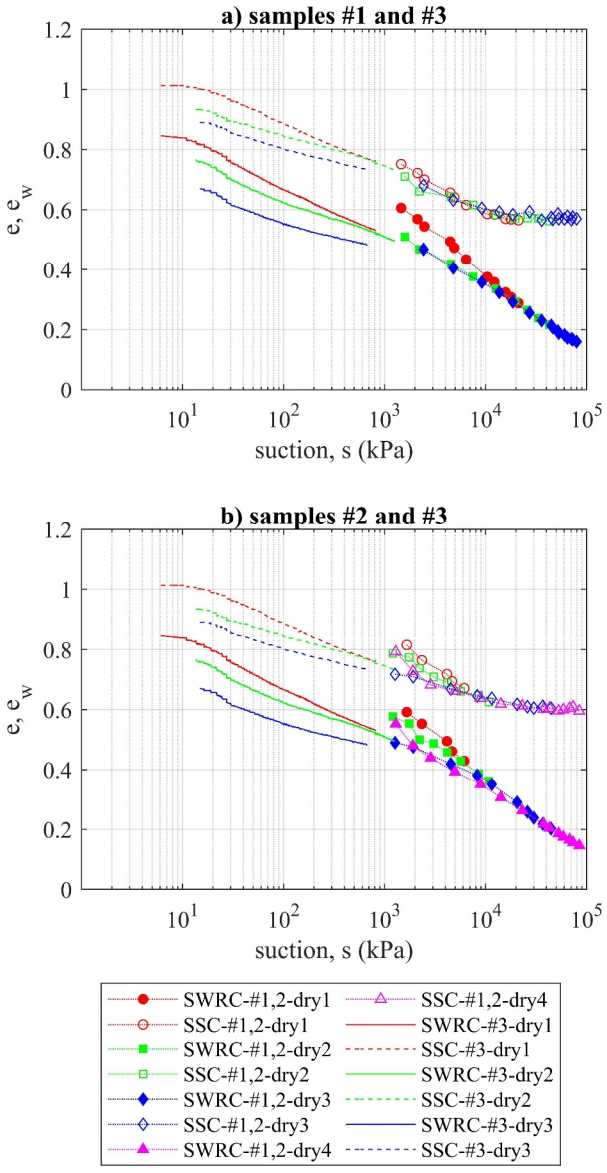

Fig. 4. Drying soil water retention curves (SWRC) and soil shrinkage curves (SSC) of samples #1, #2, and #3.

For variations of water ratio in the proportional shrinkage zone of the SSC (Fig. 2), the void ratio variation divided by the water ratio variation approximates 1 (Eq. 2). Also in this range, SSC slope in Figure 4 is given by Equation 3, where m can take the values reported in Table 3. As the slope of the SWRC in terms of water ratio is greater in absolute value than the slope of the SSC in Figure 4, a decrease of the degree of saturation at a constant rate is observed (Fig. 5).

$$\partial e/\partial log_{10}s \approx m \quad (3)$$

The variations of void ratio with water content seems to indicate reversible deformations in the proportional shrinkage zone of the SSC (Fig. 2), however, the SSC in Figure 4 always show irreversible deformations for a given suction (stress state) with subsequence cycles. This change comes as a consequence of the shift observed in the SWRCs in Figure 3, from which one could infer that the clay particles arrangement has changed [10, 11].

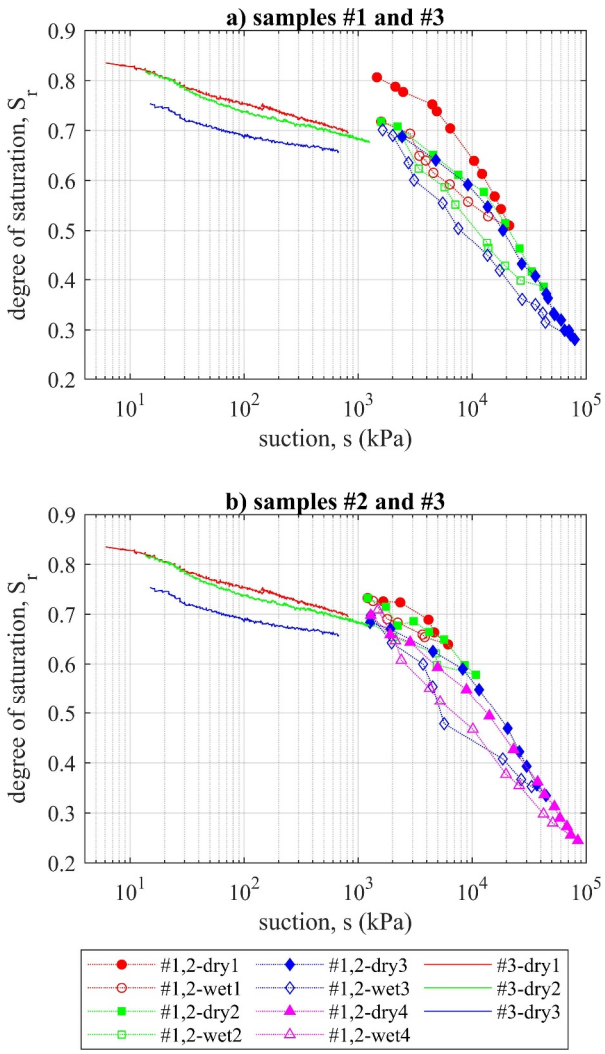

Fig. 5. Soil water retention curves in terms of degree of saturation of samples #1, #2, and #3.

In the residual shrinkage zone, the SSC becomes less steep, and the SWRC in terms of degree of saturation presents a change of slope (Fig. 5). Once the SDL

encounters the PDL, the SWRC in terms of degree of saturation is solely governed by the SWRCs presented in Figure 3 as no further changes of void ratio are observed (zero shrinkage zone). Therefore, the change of slope observed in the SWRCs in terms of degree of saturation coincides with the yielding point of the drying SWRC in terms of water ratio, which is within the residual shrinkage zone.

As the yielding point progresses towards lower suctions, volumetric deformations occur until progressively lower water ratios are reached, for which a decrease of the shrinkage limit is observed in Figure 2 (samples #1 and #2). In this way, the shift in the SSC and the accumulation of volumetric deformations results from (i) the decrease in ability of the soil to hold suction upon redrying, observed in the difference of slopes of the PDL and SDL, and from (ii) drying beyond the yielding point.

These observations have consequences on the expected behaviour of soil in a climate change scenario. As more extreme weather events become more frequent, the extreme droughts may lead the soil to dry beyond its previous yielding point, for which the suction that the soil can hold upon wetting will be reduced. There is also the potential for the suction to be lower within the following dry period.

4 Conclusions

In the present study, Soil-Water Retention Curves (SWRCs) and Soil Shrinkage Curves (SSCs) were measured on compacted high plasticity London Clay samples. The samples, subjected to suction cycles of different ranges, experienced accumulation of deformations with subsequent cycles.

The SSC was observed to be characterized by three different zones, in which the soil samples only manifested changes when cycled below the shrinkage limit. However, further examination of the SWRCs showed that all samples presented accumulation of deformations with progressive increase of the number of cycles as a consequence of a reduction of the ability of the soil to hold suction.

An upper boundary to the drying SWRCs was identified as the Primary Drying Line (PDL). Subsequent drying SWRCs are initially less steep than the PDL, described by the Scanning Drying Line,

The work presented is an output of the ACHILLES programme grant (programme grant number EP/R034575/1) funded by the UK Engineering and Physical Sciences Research Council (EPSRC).

References

1. M. North, T. Farewell, S. Hallett, A. Bertelle, Remote Sens. **9**, 922 (2017)
2. K.M. Briggs, F.A. Loveridge, S. Glendinning, Eng. Geol. **219**, 107–117 (2017)
3. H. Postill, N. Dixon, G. Fowmes, A. El-Hamalawi, W.A. Take, Can. Geotech. J. **57**, 1265–1279 (2020)
4. K.M. Briggs, T.A. Dijkstra, S. Glendinning, *Evaluating the Deterioration of Geotechnical Infrastructure Assets Using Performance Curves*, in Proceedings International Conference on Smart Infrastructure and Construction (2019)
5. R.A. Stirling, D.G. Toll, S. Glendinning, P.R. Helm, A. Yildiz, P.N. Hughes, J.D. Asquith, Géotechnique **71**, 957-969 (2020)
6. G. Liu, D.G. Toll, L. Kong, J.D. Asquith, Geotech. Test. J. **43**, 464-479 (2019)
7. A. Azizi, G. Musso, C. Jommi, Can. Geotech. J. **57**, 100–114 (2020)
8. A.S. AI-Homoud, A.A. Basma, A.I.H. Malkawi, M.A. Al Bashabsheh, J. Geotech. Eng. **121**, 562–565 (1995)
9. A.R. Estabragh, B. Parsaei, A.A. Javadi, Soils Found. **55**, 304–314 (2015)
10. J. Kodikara, S.L. Barbour, D.G. Fredlund, *Changed in clay structure and behaviour due to wetting and drying*, in Proceedings 8th Australia New Zealand Conference on Geomechanics (1999)
11. A. Dif, W. Bluemel, Geotech. Test. J. **14**, 96-102 (1991)
12. S. Tripathy, K.S. Subba Rao, Geotech. Geol. Eng. **27**, 89–103 (2009)
13. BS 1377 - Methods of test for soils for civil engineering purposes, British Standards Institution, London, UK (1990)
14. J.Y. Wang, P.N. Hughes, C.E. Augarde, *CBR strength of London Clay reinforced with polypropylene fibre*, in Proceedings of the XVII ECSMGE (2019)
15. S.D.N. Lourenço, PhD Thesis, Durham University (2008)
16. S.D.N. Lourenço, D. Gallipoli, D.G. Toll, C.E. Augarde, F. Evans, Can. Geotech. J. **48**, 327-335 (2011)
17. X. Peng, R. Horn, Soil Sci. Soc. Am. J. **77**, 372–381 (2013)
18. B. Lin, A.B. Cerato, Bull. Eng. Geol. Environ. **72**, 61–70 (2013).
19. D.G. Toll, *A conceptual model for the drying and wetting of soil*, in Proceedings of the First International Conference on Unsaturated Soils (1995)
20. E. Romero, J. Vaunat, *Retention curves of deformable clays*, in Proceedings of an International Workshop on Unsaturated Soils, Experimental Evidence and Theoretical Approaches in Unsaturated Soils (2000)
21. E. Birle, D. Heyer, N. Vogt, Acta Geotech. **3**, 191–200 (2008)